



**GEOLOGICAL SURVEY OF CANADA
OPEN FILE 6542**

Analysis of Well Logs from the Nechako Basin

C.J. Mwenifumbo and A.L. Mwenifumbo

2010



Natural Resources
Canada

Ressources naturelles
Canada

Canada



**GEOLOGICAL SURVEY OF CANADA
OPEN FILE 6542**

Analysis of Well Logs from the Nechako Basin

C.J. Mwenifumbo and A.L. Mwenifumbo

2010

©Her Majesty the Queen in Right of Canada 2010

This publication is available from the Geological Survey of Canada Bookstore
(http://gsc.nrcan.gc.ca/bookstore_e.php).
It can also be downloaded free of charge from GeoPub (<http://geopub.nrcan.gc.ca/>).

Mwenifumbo, C.J. and Mwenifumbo, A.L., 2010. Analysis of well logs from the Nechako Basin; Geological Survey of Canada, Open File 6542, 36 p.

Open files are products that have not gone through the GSC formal publication process.

Table of Contents

1. Introduction
2. Well Locations
3. Well Log Analysis
 - 3.1. CANHUNTER ESSO Nazko B-16-J/93-B-11
 - 3.1.1 Geophysical Characteristics of Lithology
 - 3.1.2. Physical Rock Property Distributions
 - 3.1.2.1. Univariate Data Distributions
 - 3.1.2.2. Bivariate Data Distributions
 - 3.1.3. Electrical and Acoustic Properties
 - 3.2. Honolulu Nazko A-4-L/93-B-11
 - 3.2.1 Geophysical Characteristics of Lithology
 - 3.2.2. Physical Rock Property Distributions
 - 3.2.2.1. Univariate Data Distributions
 - 3.2.2.2. Bivariate Data Distributions
 - 3.2.3. Electrical and Acoustic Properties
 - 3.3. Hudson's Bay Redstone C-75-A/93-B-4
 - 3.3.1. Geophysical Characteristics of Lithology
 - 3.3.2. Physical Rock Property Distributions
 - 3.3.2.1. Univariate Data Distributions
 - 3.3.2.2. Bivariate Data Distributions
 - 3.3.3. Electrical and Acoustic Properties
4. Conclusion
5. Acknowledgements
6. References

Abstract

Physical rock properties from wireline logs acquired in several wells that intersect volcanic and sedimentary rocks in the Nechako Basin have been compiled. Different rock types can be classified based on their distinct geophysical rock property characteristics. Porosity, resistivity, density, compressional velocities and acoustic impedance of volcanic rocks are distinctly different from those of sedimentary rocks suggesting that they can be successfully imaged by geophysical techniques such as seismic, magnetotelluric and gravity.

Empirical relationships between porosity, resistivity, density and compressional velocities were established. These relationships provide a means of comparing models from datasets acquired from surface seismic, magnetotellurics and gravity measurements.

1. Introduction

Exploration for oil and gas in the Nechako basin has been ongoing since 1960 (Ferri and Riddell, 2006). Several geophysical methods have been used in exploring for these resources including seismic (the work horse in the oil and gas industry), electrical (mainly magnetotelluric, MT) and gravity. The geology and structure in the basin is fairly complex and the prospective resource rocks (conglomerates and sandstones) are often overlain by thick volcanic cover with varying physical rock properties.

In this report we look at two issues, from a physical rock property perspective, which arise during exploration for oil and gas in the Nechako basin.

Imaging through thick volcanic cover

- What are the physical rock properties of the various formations (rock units) in the basin?
- With respect to physical rock properties, are there contrasts and are these significant enough to allow imaging of the different formations and resource rocks?
- Is there one physical rock property that best characterizes the sedimentary sequences (resource rocks) versus the overlying volcanic rocks?

Reconciling Models from Different Geophysical Datasets

- Seismic, electrical and gravity employ different physical rock properties. These are acquired at different scales and resolution. Integrating geophysical/geological models generated from these datasets is quite a challenge.
- Is there any relationship between resistivity and velocity/acoustic impedance, resistivity and density?

As part of the TGI-3 Cordillera project, well logging data from several wells in the Nechako basin were analyzed and compiled. These data included natural gamma ray, resistivity, density, compressional wave velocity (P-wave velocity) and neutron porosity. Not all of these geophysical parameters were acquired in all the wells. Poor quality well logs from some of the wells were not utilized in the analysis.

We analyzed the physical rock properties mainly, resistivity and acoustic (density, compressional wave velocity (V_p) and the computed acoustic impedance ($V_p * \text{density}$), from three wells. The well log data were acquired through a subscription from Divestco (Divestco – EnerGISite.com, 2007).

2. Well Locations

Although we had access to geophysical logs from nine wells, we focused our analysis on four wells based on the data quality, availability of the critical logs (electrical resistivity, velocity, density and porosity) and on the intersected lithology. Figure 1 shows the location of the wells analyzed in this report.

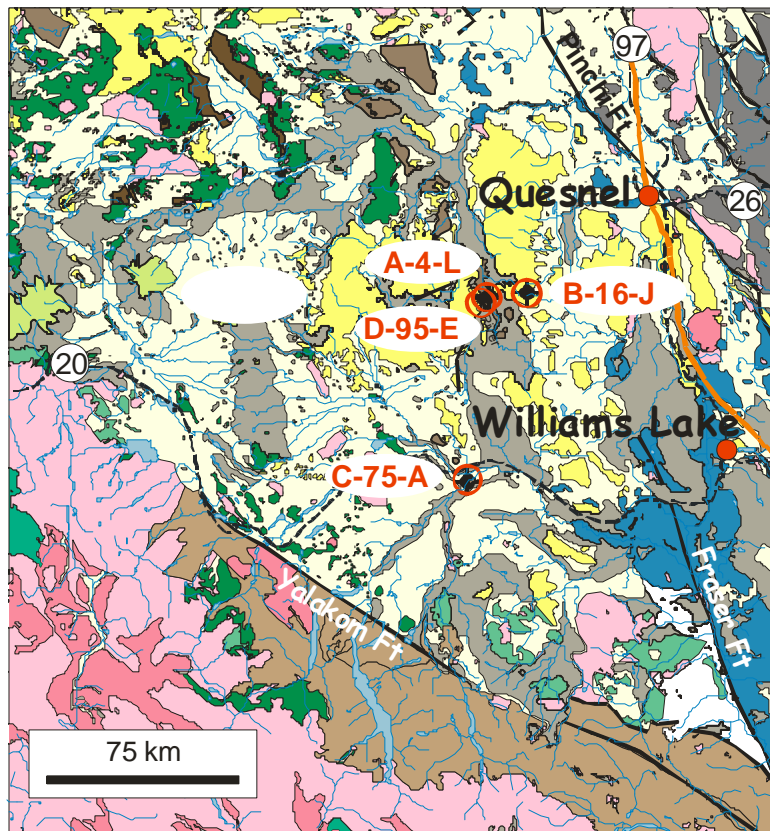


Figure 1: Well locations in Nechako Basin.

3. Well Log Analysis

3.1 CANHUNTER ESSO Nazko B-16-J/93-B-11

3.1.1 Geophysical Characteristics of Lithology

B-16-J/93-B-11 well was drilled by Canadian Hunter Exploration and the stratigraphy intersected consists of five major lithology packages (from top to bottom): 1) Eocene-Oligocene volcanic flows of the Endako formation; 2) a conglomerate/tuff/sandstone sequence; 3) conglomeratic sandstone; 4) volcanic tuffs with minor flows and volcanoclastics; and 5) Triassic basic (basalts) volcanic flows (Ferri and Riddell, 2006). This well represents a sequence of rocks, typical of the problem of imaging prospective oil and gas source rocks (conglomerate and sandstone) through a thick volcanic cover.

There is a fairly comprehensive suite of well logs from well B-16-J/93-B-11. Figure 2 shows the gamma, resistivity, porosity, density, velocity and computed acoustic impedance logs. Lithology is superimposed on the well logs to enhance visual correlation between geology and geophysics.

The geophysical characteristics of the different rock units are summarized below.

- The gamma ray log clearly identifies the five lithology packages. Extremely low levels of radioactivity are observed in the basalts. The volcanic tuffs overlying the basalts exhibit the highest radioactivity. The conglomeratic sandstones exhibit very uniform activity.
- Resistivity also reflects lithology changes. The volcanic flows exhibit very high resistivity with the highest being observed in the basalt flows. The claystone/shale overlying the basalts has low resistivity. Variations in resistivity in the conglomeratic sandstone reflect the ratio of sandstone to conglomerate and the degree of cementation (porosity) within the different layers.
- The porosity log response is a mirror image of the resistivity log; high resistivity correlates with low porosity, and vice versa, because these physical parameters are primarily a function of pore space and pore fluid salinity.
- The density, velocity and acoustic impedance logs have similar responses in all five lithology packages and correlate well with resistivity.

All the physical rock properties show very anomalous characteristics in the conglomeratic tuffaceous layer (1640 – 1730 m) overlying the volcanic tuffs and that are immediately overlain by the conglomeratic sandstone. The porosity in this unit is very high, while the resistivity, density, velocity and acoustic impedance are extremely low. This rock unit is an excellent geophysical marker and could be used for verifying and/or constraining models developed through resistivity and seismic inversions. Also the tuffaceous layer (1320 – 2390 m) overlying the Cache Creek volcanic flows exhibits anomalously low resistivity, density, velocity and acoustic impedance. The neutron porosity is high.

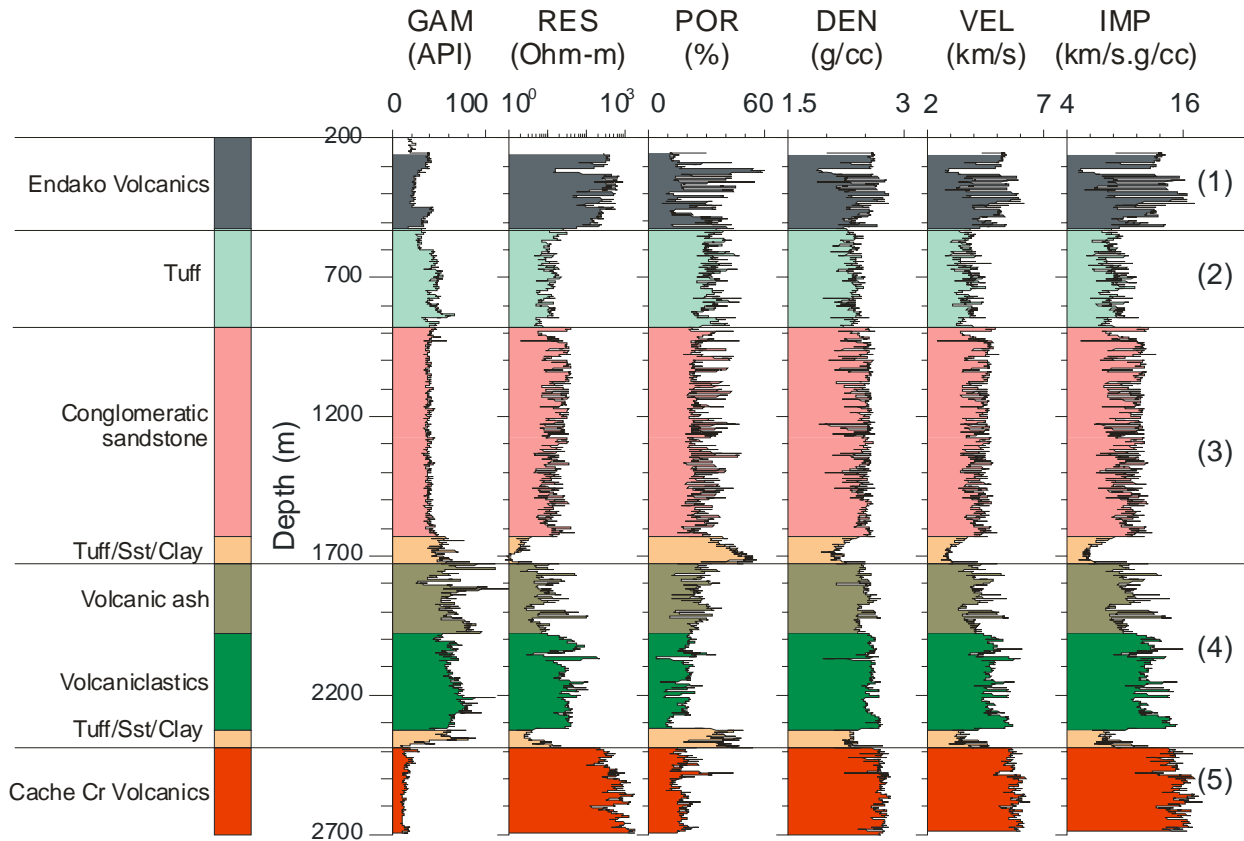


Figure 2: Gamma, resistivity, porosity, density, velocity and acoustic impedances logs from B-16-J/93-B-11 well. The lithology (Well History report on Canhunter ESSO Nazko b-16-J/93-B-11, 1981) is superimposed on the well logs. The numeric values on the right of the figure represent the rock packages described in the text. GAM= gamma, RES = Resistivity, POR = Porosity, DEN = Density, VEL = Velocity, IMP= acoustic impedance (VEL*DEN). Rock package (4) has been subdivided in two units based on the geophysical characteristics.

3.1.2 Physical Rock Property Distributions

3.1.2.1 Univariate Data Distributions

Box-and-whisker plots showing distributions within the different lithology units for five parameters (gamma-ray, resistivity, porosity, density, velocity and the computed acoustic impedance) are shown in Figure 3. The box-and-whisker plot is a graphical statistical summary of data distribution. The boxes are bounded by the 25th (lower hinge) and the 75th percentiles (upper hinge). The notch locates the median (50th percentile) and its 95% confidence bounds. The whiskers, lines drawn from the lower and upper hinges, represent data within $1.5 \times \text{IQR}$ from the hinges, where IQR is the inter-quartile range or box length. Data beyond the whiskers (outliers) are removed from these plots.

The gamma ray signature of the Cache Creek volcanic flows is distinctly different from the shallow Endako volcanic flows (Figure 3a). Cache Creek volcanics exhibit the lowest radioactivity of all the lithology intersected in the well. The volcanoclastics exhibit the highest radioactivity. The radioactivity in these formations is primarily a function of the concentrations of the radioelement potassium. The volcanoclastics, volcanic ash and tuffs show wide distributions in their radioelement content as indicated in the box length. The radioelement distribution in the conglomeratic sandstone and the Cache Creek volcanics are quite tight (Figure 3a) and fairly uniform (Figure 2).

Both the Endako and the Cache Creek volcanics show extremely high resistivities, $>100 \text{ Ohm-m}$ (Figure 3b). The volcanic ash, volcanoclastics and conglomeratic sandstones have resistivities lower than 50 Ohm-m .

The porosity and density distributions show an inverse relation in all the lithology assemblages; porosity increasing with decreasing density (Figures 3c and 3d). The density distribution in the Endako volcanics is quite variable (box length $\sim 0.3 \text{ g/cc}$). Fairly tight distributions in both the porosity and density are observed in the Cache Creek volcanics. The velocity and acoustic impedance (Figures 3e and 3f) show similar characteristics in their distributions. The asymmetry in the box-whisker plots relative to the median indicates that the distributions are skewed and not normal. Tables 1 and 2 show the mean and median values for the different lithologies depicted in the box-and-whisker plots.

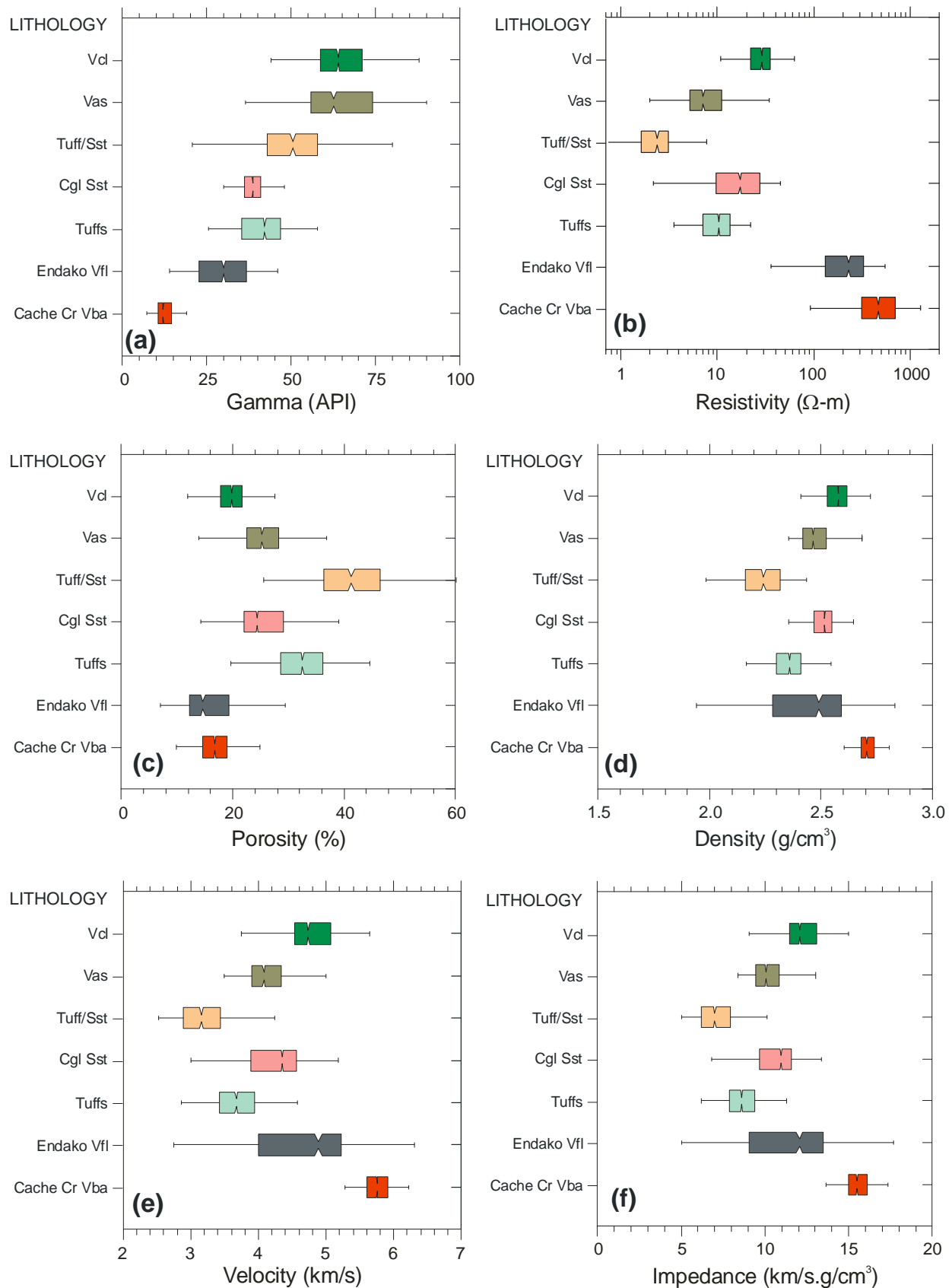


Figure 3: Box-and-whisker plots of (a) gamma, (b) resistivity, (c) porosity, (d) density, (e) velocity and (f) acoustic impedance. Vba – basic volcanic flows, Vcl – volcanoclastics, Vas –

volcanic ash, Vtu – volcanic tuffs, Vfl – volcanic flows, Sst – sandstone, Cgl/ssst – conglomeratic sandstone, Cgl – conglomerate

Table 1: Statistical summary of the distribution of gamma, resistivity and porosity for the various lithology packages intersected in well B-16-J/93-B-11

Lithology	Gamma		Resistivity		Porosity	
	Mean	Median	Mean	Median	Mean	Median
Volcaniclastics	13.14	12.89	11.36	10.58	17.76	12.15
Volcanic ash	29.82	29.99	18.96	18.96	26.12	10.03
Tuff/Sandstone/clay	41.33	42.33	5.42	2.53	32.90	7.22
Conglo. sandstone	38.81	38.66	12.91	7.41	27.02	10.92
Tuffs	49.82	50.52	36.42	29.64	40.92	8.58
Endako Volcanics	67.32	63.80	263.21	240.01	24.43	12.07
Cache Creek Volcanics	64.78	63.90	655.13	50843	17.87	15.46

Table 2: Statistical summary of the distribution of density, velocity and acoustic impedance for the various lithology packages intersected in well B-16-J/93-B-11

Lithology	Density		Velocity		Impedance	
	Mean	Median	Mean	Median	Mean	Median
Volcaniclastics	2.57	2.57	5.71	5.73	12.43	12.15
Volcanic ash	2.48	2.47	4.62	4.88	10.31	10.03
Tuff/Sandstone/clay	2.24	2.24	3.70	3.68	6.70	7.22
Conglo. sandstone	2.47	2.51	4.23	4.35	10.47	10.92
Tuffs	2.34	2.35	3.31	3.22	8.66	8.58
Endako Volcanics	2.42	2.47	4.15	4.05	11.37	12.07
Cache Creek Volcanics	2.69	2.70	4.84	4.75	15.38	15.46

3.1.2.2 Bivariate Data Distributions

Gamma versus Resistivity

Figure 4 shows the gamma-resistivity cross-plot (resistivity plotted on logarithmic scale) and the 2D kernel density distribution for well B-16-J/93-B-11. The kernel density distribution employs a kernel method of probability density estimation (Mwenifumbo, 1993). The standard way of presenting distributions, at least for univariate data, is the histogram format. This format of data presentation cannot be easily extended to bivariate or multivariate data and hence the adoptions of the kernel method of density estimation.

The data in the cross-plot have been grouped according to the major lithology packages (Ferri and Riddell, 2006; Well History report on Canhunter ESSO Nazko b-16-J/93-B-11, 1981).

- Most of the sandstone and conglomeratic sandstones cluster in the field of gamma <50 and resistivity <50 ohm-m. Since changes in gamma-ray activity are related to variations in concentrations of the radioelement potassium, the observed clusters can be correlated to changes in the percentage of potassium bearing minerals within the individual rock units.
- The Cache Creek and Endako volcanic flows have low gamma ray activity and the highest resistivities. There are two distinct clusters visible in the Endako volcanics and the discriminating parameter is the gamma ray activity.
- The volcanoclastics (green) also exhibit two distinct groups and the discrimination between them is primarily by the resistivity.
- The conglomerates at the base of the conglomeratic sandstone have the lowest resistivity.

The 2D kernel density distribution shows two major clusters; the cluster in the high resistivity-low gamma field corresponds to the volcanic flows and the other cluster comprises mainly the sedimentary rocks.

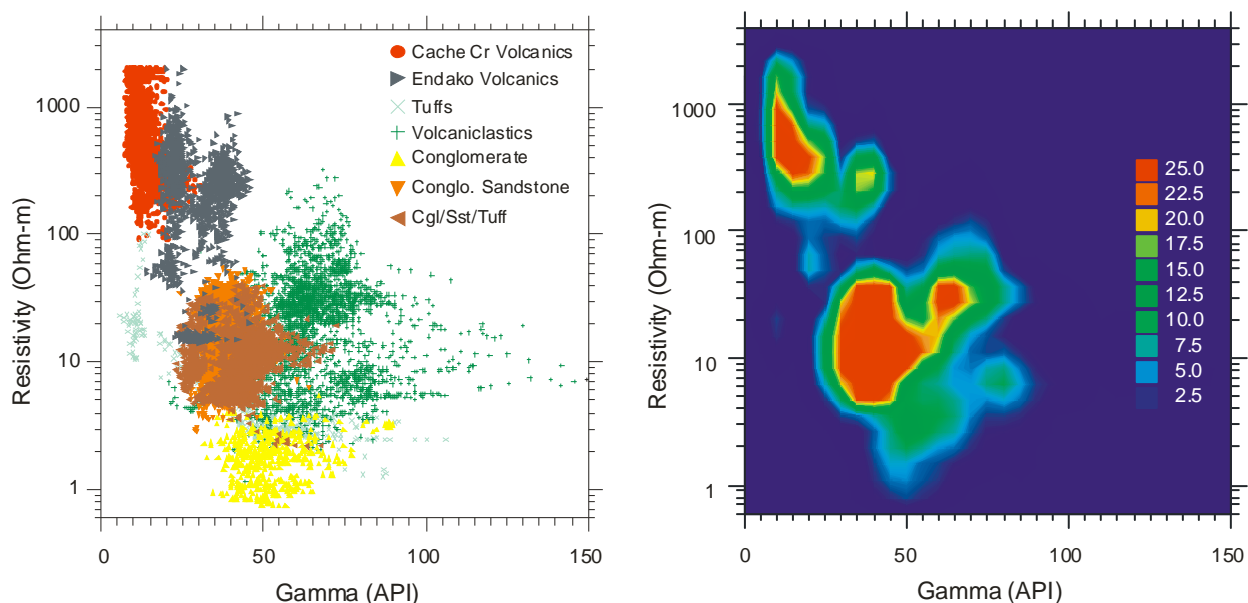


Figure 4. Resistivity-gamma cross-plot and 2D kernel density distribution. Data in the cross-plot are classified according to the major lithology/formations intersected in the well.

Density, Velocity and Resistivity as a Function of Porosity

The fundamental petrophysical parameter that controls variations in density, velocity, and resistivity in sedimentary rocks is porosity. The relationship of these parameters to porosity in volcanic and/or igneous rocks is not always straight forward. Figures 5, 6, 7, show these parameters cross-plotted with porosity from the neutron porosity log. The neutron log works well in sedimentary rocks. Hydrous minerals in volcanic and igneous rocks tend to give false high

porosity response. Also several alteration minerals, such as sericite, will give false positive neutron porosity highs.

Porosity as a Function of Density

The porosity-density cross-plot and the kernel density distribution are presented in Figure 5. The porosity decreases with an increase in density as both parameters are governed by the amount of pore space within the rocks. A regression line and empirical relationship are included in Figure 5.

The standard porosity-density relationship is given as follows

$$\phi = (\rho_{ma} - \rho_b) / (\rho_{ma} - \rho_f)$$

Where ρ_{ma} is matrix or grain density, ρ_b is bulk density and ρ_f is the density of the pore fluid. If we let the fluid density is 1 and the matrix density is 2.65 (quartz sandstone) then the above equation reduces to

$$\phi = (1.606 - 0.606x \rho_b) \times 100$$

The constant and the coefficient are a bit different from those determined from the regression line. The differences are primarily due the assumed matrix densities and fluid densities.

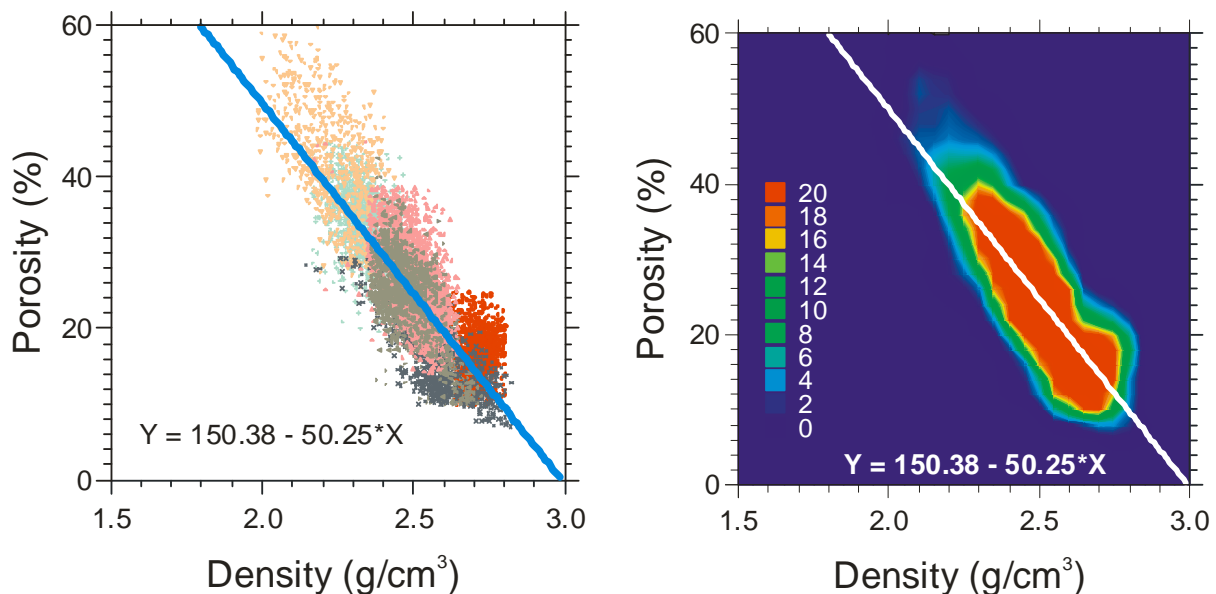


Figure 5. Porosity-density cross-plot and the 2D-kernel density estimate plot. The solid line represents a linear regression line fit to the data.

The broad-banded nature of the data distribution (Figure 5b) may reflect differences in the sample volume of each of these two parameters and also minor discrepancies in the observation depth for each sample.

Porosity as a Function of Velocity

The porosity-velocity cross-plot and the kernel density distribution are presented in Figure 6. The porosity decreases with an increase in velocity. Velocity variations in both sedimentary and volcanic rocks are highly governed by porosity. The kernel density distribution shows that the Cache Creek volcanics are outliers in this relationship. This suggests that lithology plays a significant part in the porosity-velocity relationship. Two regression lines are presented on both the cross-plot and the kernel density distribution; one with all the datasets in the regression (black line on cross-plot and white on the kernel density plot) and the other line (blue) fitted to a dataset without the Cache Creek volcanics. The empirical relationships are also presented in Figure 6.

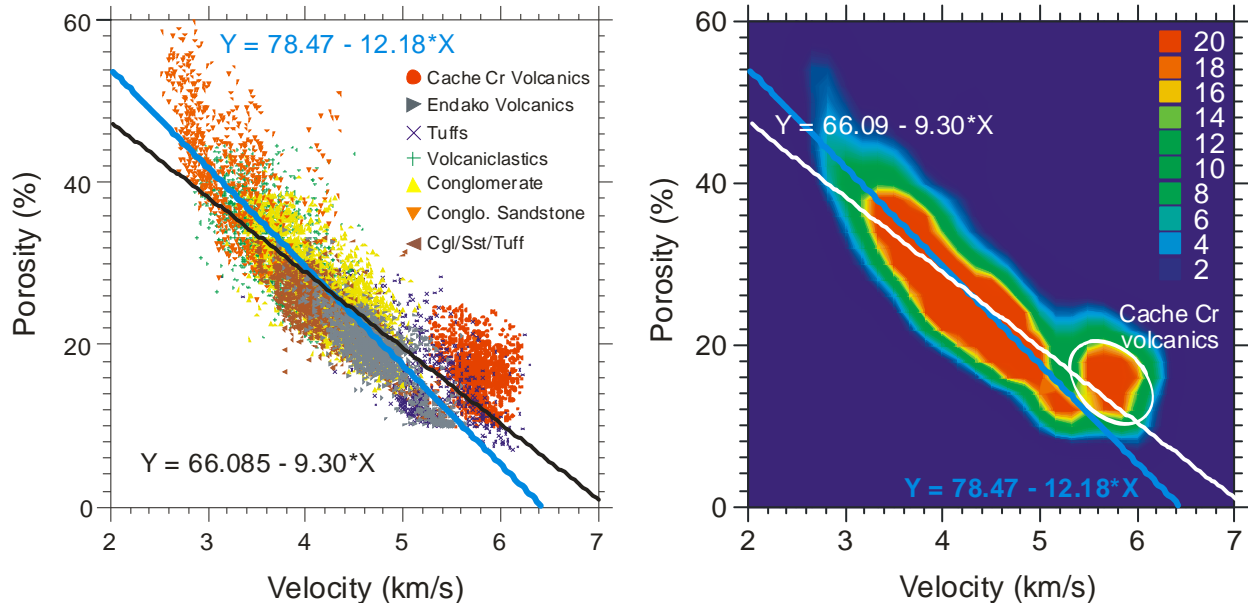


Figure 6: *Porosity-velocity cross-plot and the 2D kernel density distribution*

Empirical porosity-velocity relations:

For all lithologies

$$\phi = 66.09 - 9.30 \times V_p$$

For lithologies excluding the Cache Creek volcanic flows

$$\phi = 78.47 - 12.18 \times V_p$$

Porosity as a Function of Resistivity

The porosity-resistivity cross-plot and the kernel density distributions (Figure 7) show porosity decreasing with increases in resistivity for all lithologies. Both the cross-plot and the kernel density distribution show two main clusters in the dataset. The Endako and Cache Creek volcanic flows form a cluster in the high-resistivity low-porosity field (cluster B) that is well separated from the rest of the rock units. The sedimentary, conglomeratic sandstone and volcanoclastics cluster in the low-resistivity field (cluster A). The dataset indicates that lithology contributes significantly to the porosity-resistivity relationship. Establishing a porosity-resistivity relationship for data from all the lithology would not provide a correct relationship. Resistivity changes in the highly resistive volcanic flows (200 – 2000 Ohm-m), appear not to be related to porosity (cluster B).

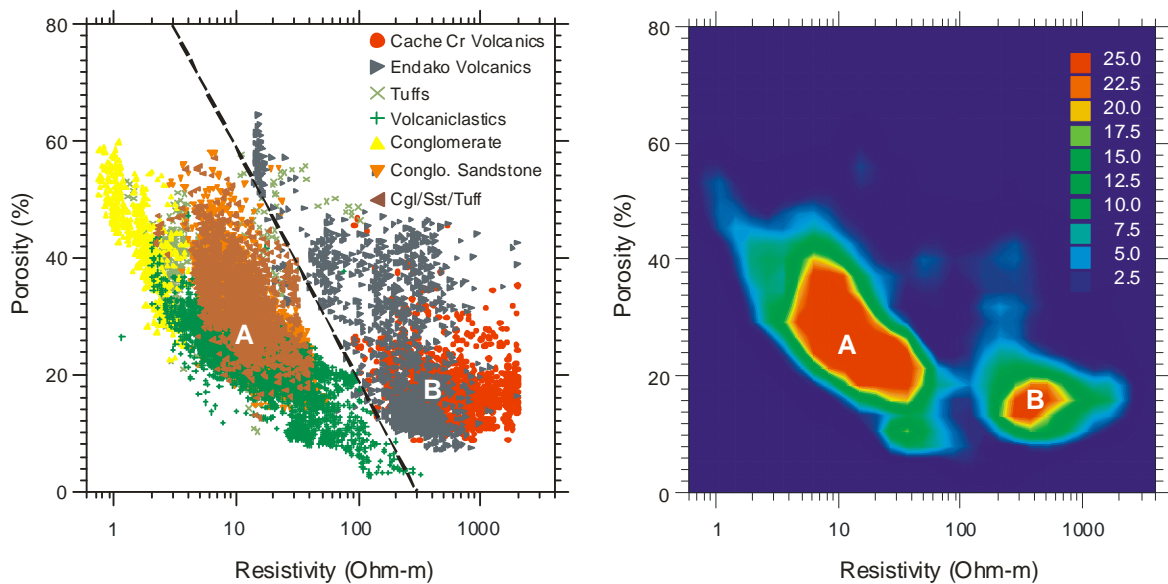


Figure 7: Porosity-resistivity cross-plot (a) and its 2D kernel density distribution

Acoustic Properties

Velocity as a Function of Density

Several relationships between velocity and density have been reported in the literature (Brocher, 2005). These empirical relationships have been established for different geological environments (sedimentary, metamorphic and igneous) due to the following:

- (a) Seismic velocities vary with mineral content, lithology, porosity and pore fluid saturation. In igneous and metamorphic rocks with minimal porosity, seismic velocity increases with increasing mafic mineral content. In sedimentary rocks, effects of porosity and degree of cementation are more important, and seismic velocity relationships are complex.
- (b) Density variations are primarily a function of lithology (chemical composition, grain density) and porosity.

The most well known relationship between velocity and density is the Nafe-Drake curve. A fairly comprehensive list of relationships is given in Brocher, 2005.

Figures 8 and 9 show the velocity-density cross-plots for the sedimentary rocks and the volcanic rocks, respectively. The Nafe-Drake curve and Gardner's rule are compared in the sedimentary cross-plot. The velocities increase with density in these rocks following both the Nafe-Drake curve and Gardner's rule for velocities between 2 and 6 km/s and for densities between 1.5 and 3 g/cc. An excellent linear relationship was established for the current data set in the volcanic rocks (Figure 9).

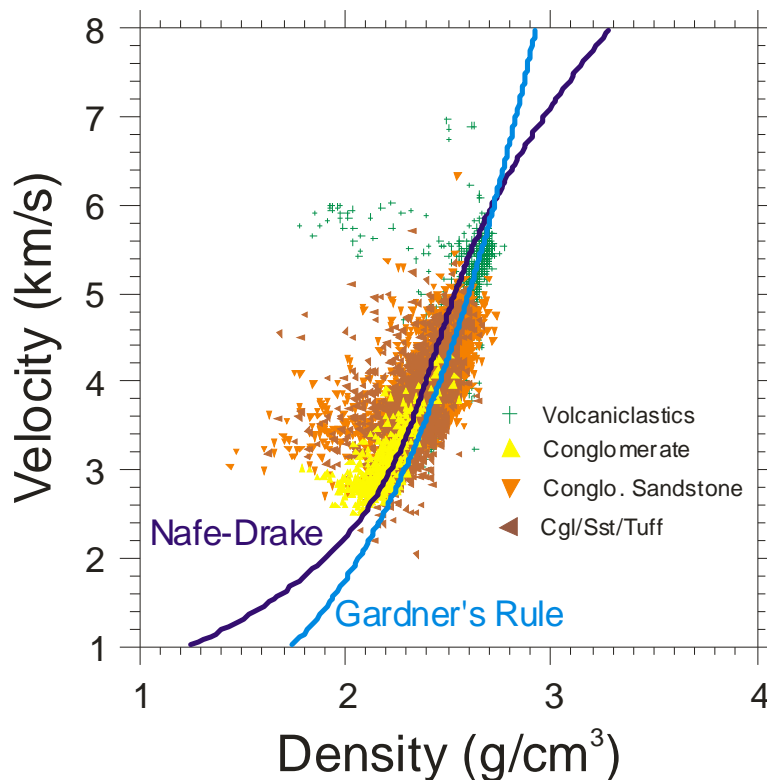


Figure 8: Velocity-density cross-plot for the sedimentary rocks (conglomerates, sandstones) and volcaniclastics. The Nafe-Drake and the Gardner's rule velocity-density relationship are presented. Conglo. = conglomerate; Cgl/Sst/Tuff = conglomerate/sandstone/tuff.

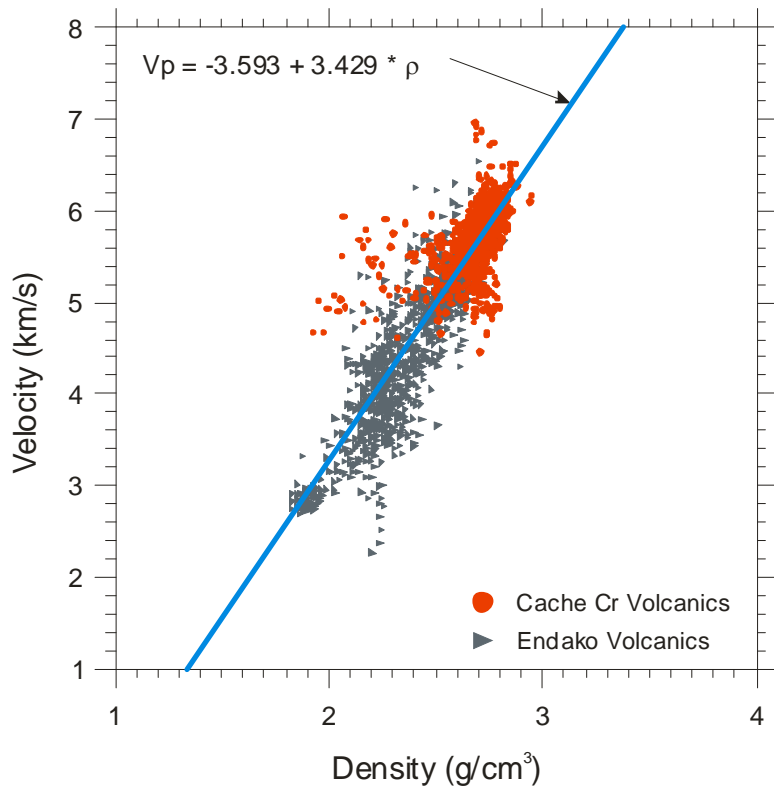


Figure 9: Velocity-density cross-plot for the volcanic flows. Red - Cache Creek volcanic flows and grey symbol - Endako volcanic flows.

The acoustic properties for all the lithologies intersected in well B-16-J are presented in the velocity-density cross-plot and the 2D kernel density distribution in Figure 10. The velocity-density distribution closely follows the Nafe-Drake curve and Gardner's rule. The relationship derived for the volcanic flows is significantly different from the Nafe-Drake relationship and Gardner's Rule.

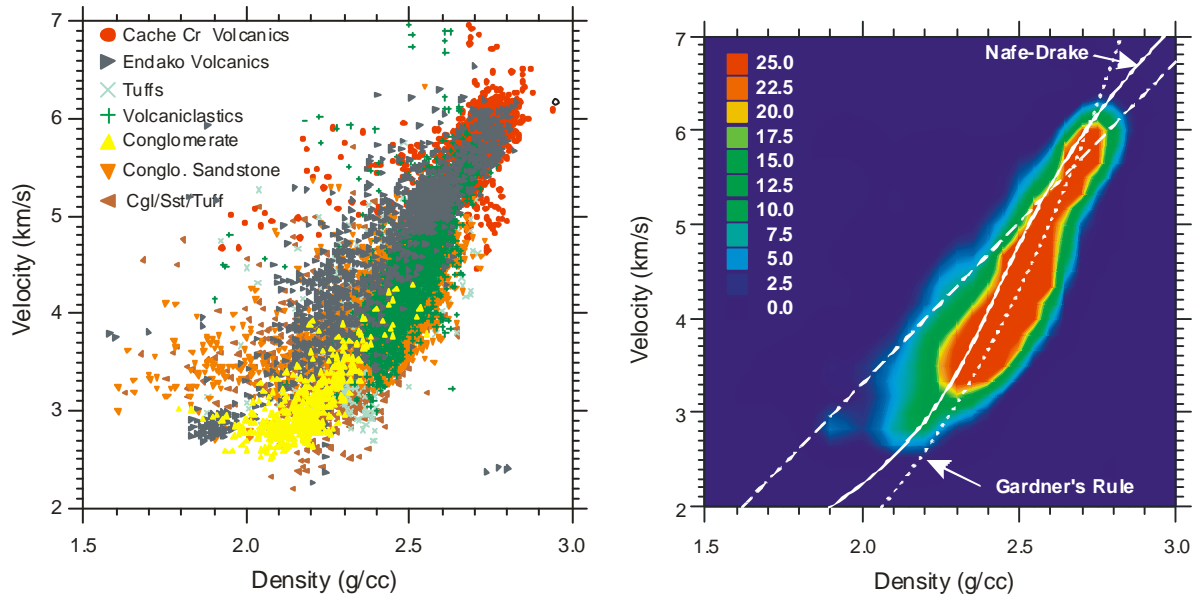


Figure 10. Velocity-density cross-plot and 2D kernel density distribution for all the lithologies in well B-16-J. The linear regression line is for the mafic volcanic flows while the Nafe-Drake and Gardner's rule are non-linear empirical rules. Cr = Creek, Conglo. = conglomerate; Cgl/Ssst/Tuff = conglomerate/sandstone/tuff.

3.1.3. Electrical and Acoustic Properties

The standard geophysical exploration method used in the oil and gas industry is seismic and the physical rock properties of interest are density, velocity and acoustic impedance (a product of density and velocity). Due to the complexity of the geological environment in the Nechako basin, other geophysical exploration tools such as magnetotellurics and gravity have been applied and are under further development to improve the targeting of potential resource rocks and structures.

In this section we examine the relationship between the electrical and acoustic properties of the volcanics and the sedimentary rocks in the Nechako basin. Understanding the relationship between these two physical rock properties will greatly improve the geology and geophysical modeling of the Nechako basin and integration of electrical and seismic datasets.

Well B-16-J/93-B-11 Esso Nazko represents an ideal lithology/stratigraphy intersection to examine the problem of how to image through a sequence of thick volcanics that overly the potential resource rocks, conglomerates/sandstone and shales. The issue is... how do we image through thick volcanic cover? Since the two main exploration tools that are currently being revisited are electrical (mainly MT) and seismic, we seek to understand the relationship between the electrical and acoustic properties of the volcanics and the potential source rocks - the conglomerates and sandstones.

We see significant changes in the resistivity and the acoustic impedance between the five major lithology packages (Figures 11). The volcanic tuff/conglomeratic and the conglomeratic sandstones show a significant contrast in resistivity and acoustic impedance. For acoustic energy reflectivity, a reflection coefficient of 0.05 or greater is considered significant (Eaton et al., 2006).

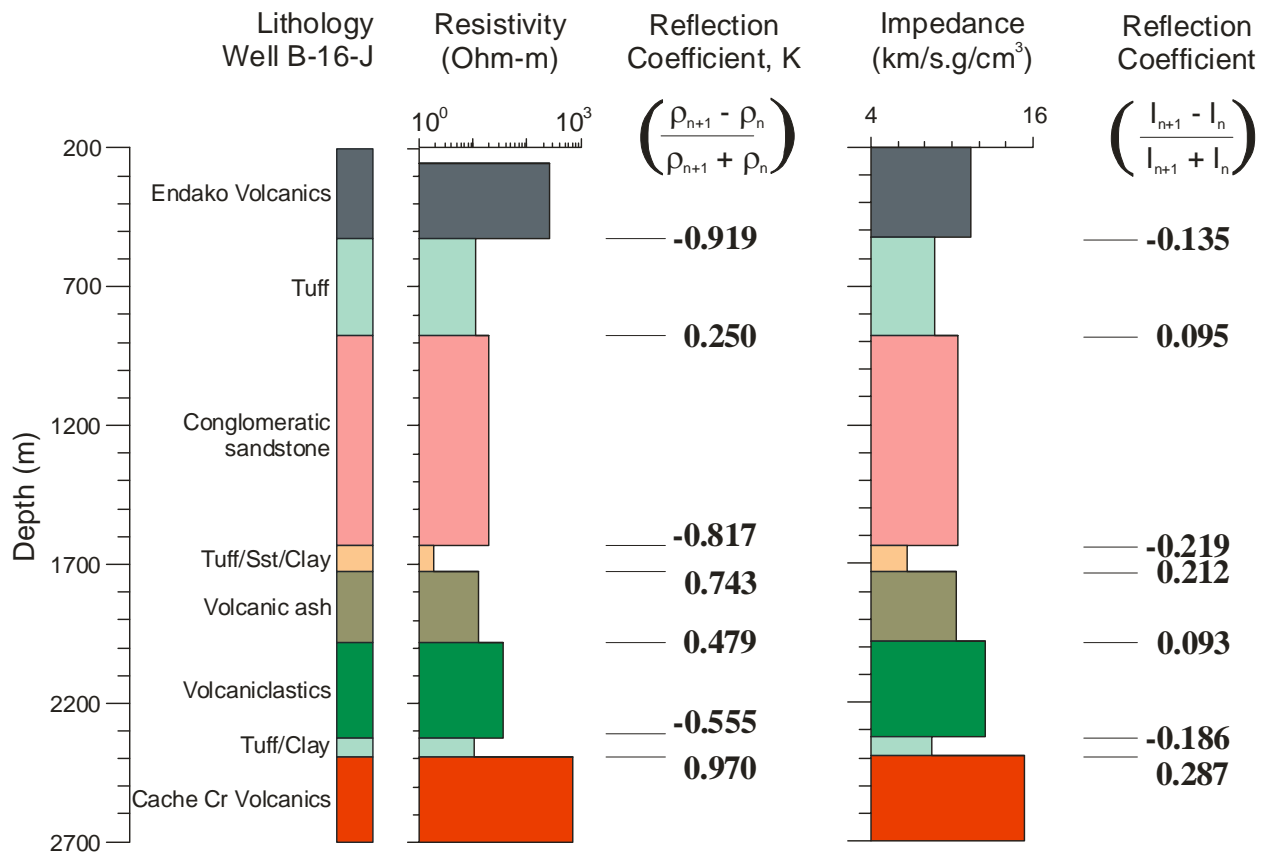


Figure 11. Resistivity and acoustic impedance log averaged according to the major lithology packages. The computed reflection coefficient at each interface is presented in the right hand column of each parameter

Resistivity as a Function of Velocity

It is important to compare geological models derived from various geophysical techniques that measure parameters differently. In the present work, we look at how geological models generated from electrical methods would compare to those generated from seismic methods. What kind of relationship exists between electrical properties (resistivity/conductivity) and acoustic properties (density and P-wave velocities)?

Figure 12 show a cross-plot and 2D kernel density distribution of resistivity as a function of velocity. The data are grouped according to the lithology in the scatter-plots. There is significant scatter in the dataset from the Endako volcanics primarily due to velocity changes. Good, positive correlation exists between the logarithm of resistivity and velocity. When we closely examine the data, we see two clusters; cluster (A) consisting of sedimentary rocks and cluster (B) in the high-resistivity high-velocity region consisting of basic Cache Creek and Endako volcanic flows. This is a similar relationship observed in the porosity-resistivity cross-plot. This observation implies that separate relationships have to be established for the volcanics and for the sedimentary rocks when converting the datasets. A log-linear regression line has been fitted to the resistivity-velocity dataset for all the lithologies and there is a good fit despite the two distinct lithology clusters.

$$\log_{10}(R) = -1.71 + 0.72 * V_p$$

This relationship between resistivity and velocity suggests that velocities can be derived from resistivity data. In addition, models generated from electrical survey data would be comparable to those generated from seismic survey data provided structural complexities are not the major controlling factors in the observed geophysical responses.

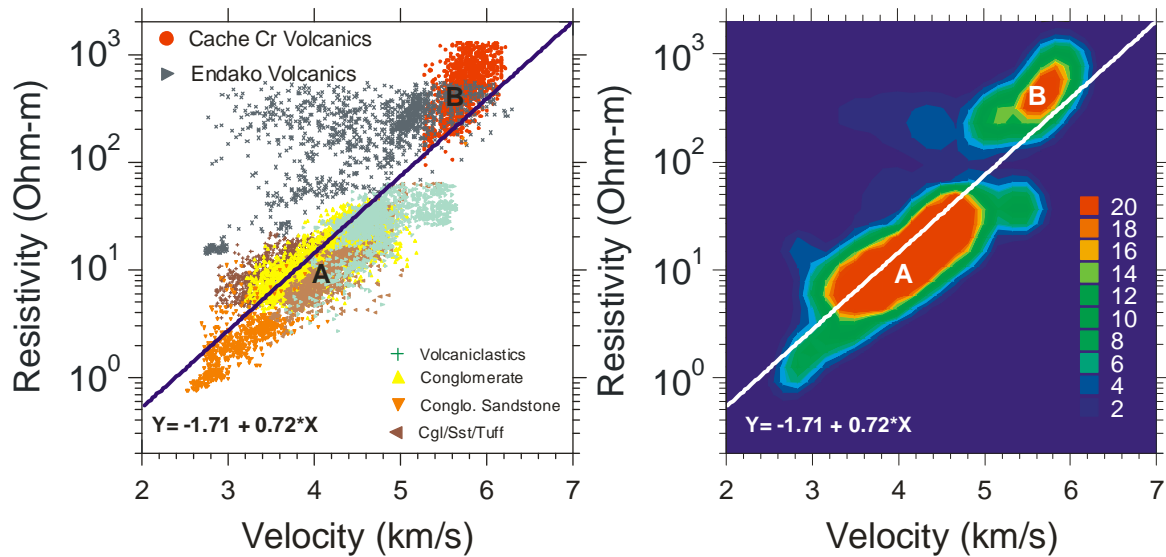


Figure 12. Resistivity-velocity cross-plot and the 2D kernel density distribution. Lithologies in cluster (A) consist of sedimentary rocks and volcaniclastics whereas those in cluster (B) comprise the Cache Creek and Endako volcanic flows. Conglo. = conglomerate; Cgl/Sst/Tuff = conglomerate/sandstone/tuff.

Resistivity as a Function of Acoustic Impedance

The resistivity-acoustic impedance cross-plot and the 2D kernel density distribution are presented in Figure 13. The observations are similar to those of the resistivity-velocity relations. Regressions of resistivity and acoustic impedance for all lithologies and for sedimentary and volcanoclastics are also presented in Figure 13.

For all lithologies

$$\log_{10} (R) = -0.903 + 0.213 * I$$

For sedimentary rocks and volcanoclastic rock assemblages

$$\log_{10} (R) = -0.529 + 0.160 * I$$

Where R = resistivity and I= acoustic impedance (velocity x density)

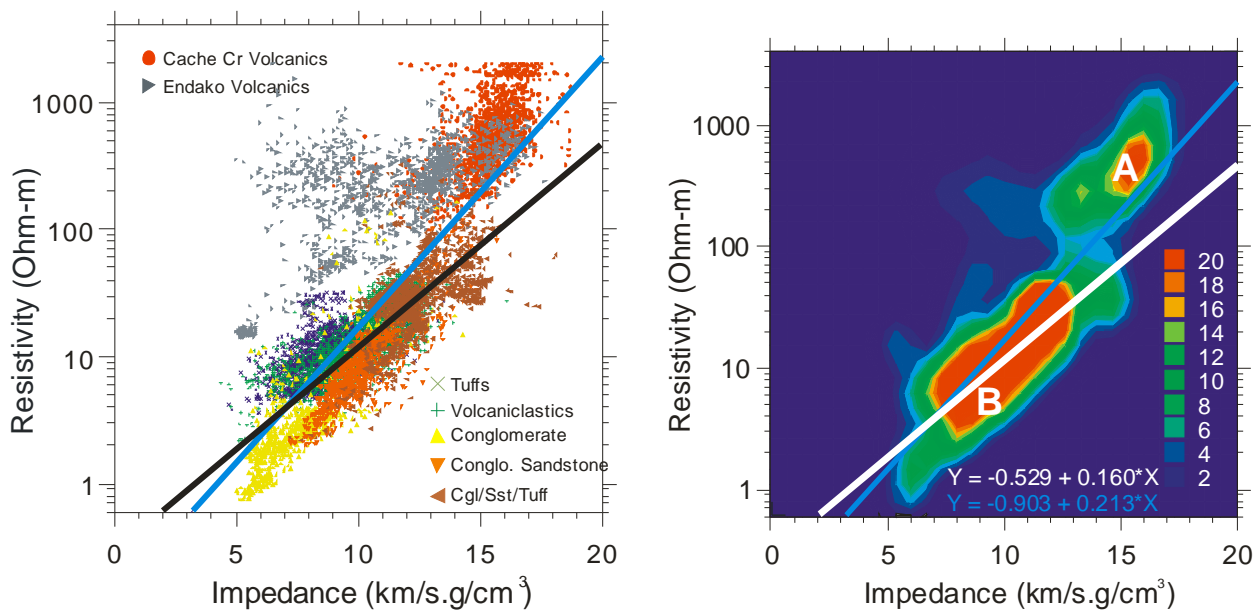


Figure 13. Resistivity-impedance cross-plot and 2D kernel density distribution. Lithologies in cluster (A) consist of sedimentary rocks and volcanoclastics, whereas those in cluster (B) comprise the Cache Creek and Endako volcanic flows. Regression line for all the lithologies (blue) and for the sedimentary and volcanoclastics (black in cross-plot, and white in the kernel density distribution). Cr. = Creek, Conglo. = conglomerate; Cgl/Ssst/Tuff = conglomerate/sandstone/tuff.

3.2. Honolulu Nazko A-4-L/93-B-11

3.2.1. Geophysical Characteristics of Lithology

The Honolulu Nazko well intersects (from top to bottom) the Taylor Creek Group and the Jackass Mountain group sedimentary sequence. This sedimentary sequence is underlain by the volcanics of the Cache Creek group (Ferri and Riddell, 2006). The Taylor Creek Group is predominantly shale with a thick conglomerate/sandstone section between 1355 and 1615 m. The Jackass Mountain Group consists of sandstone, shale and siltstone between 2100 and 2375 m.

The gamma, resistivity and velocity logs are presented for the sedimentary sequence (Figure 14). Some of the logging parameters were acquired in the Cache Creek volcanics. The Taylor Creek Group has been subdivided into several geologic units based on lithology description (Well Report, Honolulu Nazko #A-4-L, 1961) and the geophysical logs. Visual inspection of the well logs shows an excellent positive correlation between the resistivity and velocities (V_p). The high-resistivity, high-velocity lithology units correspond to the thick conglomerate/ sandstone.

There is an overall good correlation between the resistivity, velocity and the gamma log. The low gamma ray readings in the sandstone/conglomerate exhibit high resistivity and high velocities. The shales in the Taylor Creek are characterised by high gamma ray activity and relatively lower resistivity and velocity. The shale overlying the Jackass Mountain shale show relatively the same gamma ray activity, but there is a distinct difference in both the resistivities and velocities below 1980 m (lower portion of the shale has lower resistivities and lower velocities, Figure 14). It is interesting to note that the Jackass Mountain shale has distinct, higher gamma ray activity compared to the Taylor Creek shales.

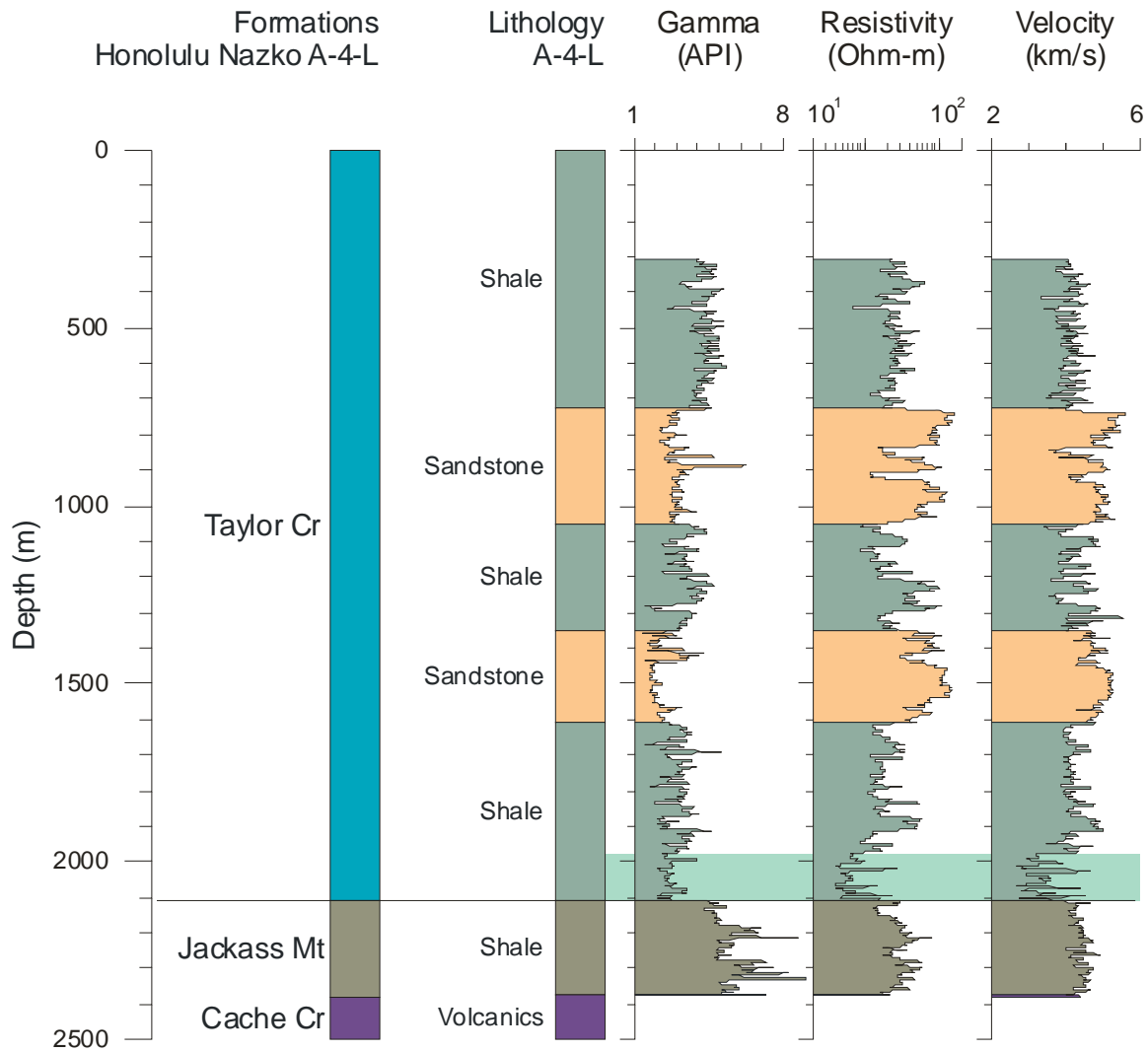


Figure 14. Gamma, resistivity and velocity logs through the Taylor Creek and Jackass Mountain Formations. The lithology is superimposed on all the three logs. The Taylor Creek shale overlying the Jackass Mountain shale with anomalously low resistivity and velocity is shaded in pale green.

3.2.2. Physical Rock Property Distributions

3.2.2.1 Univariate Data Distributions

Box and whisker plots and histograms showing distributions of resistivity, velocity and gamma in three main lithology packages; the Taylor Creek shales, Taylor Creek sandstone/conglomerate and the Jackass Mountain shales are presented in Figures 15, 16 and 17). The resistivity shows that the shales and sandstone/conglomerates in the Taylor Creek Formation are different (Figure 15). The resistivity of the Jackass Mountain shales is higher than the Taylor Creek shales but distinctly lower than the Taylor Creek sandstone/conglomerates. The velocity shows similar distribution (Figure 16). The velocity distribution in the Taylor Creek shale is negatively skewed.

The gamma data, generally used as a lithology indicator, show the Jackass Mountain group, as being very distinctive from the other lithology units (with the highest gamma activity). This high gamma ray activity is characteristic of a sedimentary sequence with a high percentage of potassic minerals and/or clays. This observation implies that the percentages of either potassic minerals or clay are higher in the Jackass Mountain shales as compared to the Taylor Group Formation

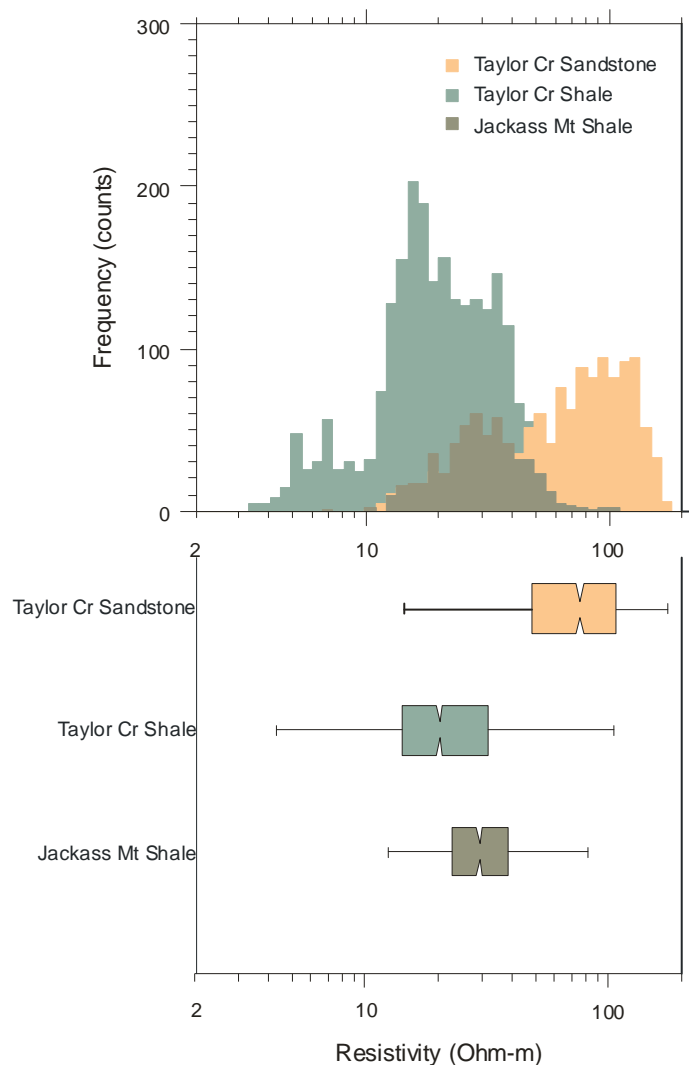


Figure 15. Histogram distributions and box-and-whisker plots of the resistivity for the Taylor Creek sandstone and shale, and for the Jackass Mountain shale in the Honolulu Nazko A-4-L well.

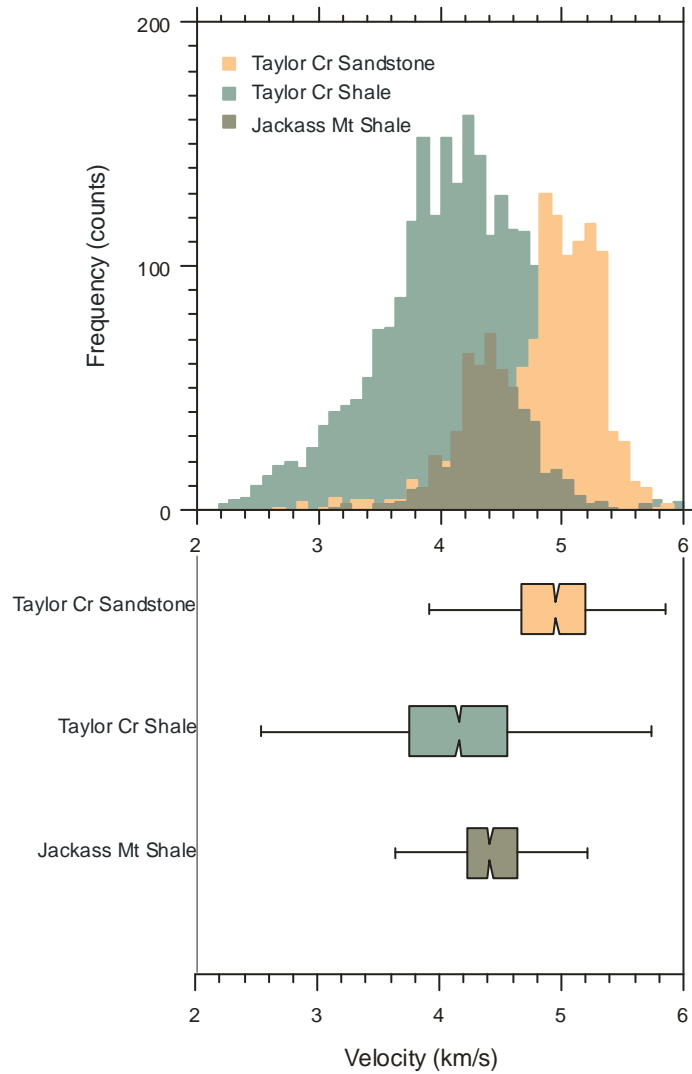


Figure 16. Histogram distributions and box-and-whisker plots of the velocity for the Taylor Creek sandstone and shale, and for the Jackass Mountain shale in the Honolulu Nazko A-4-L well.

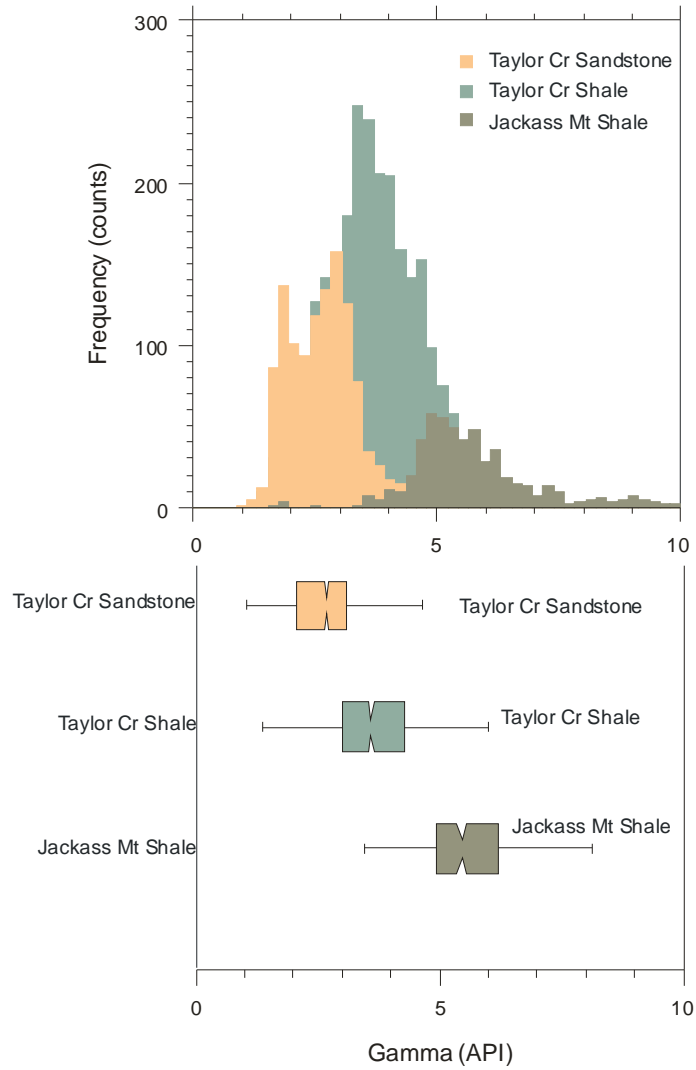


Figure 17. Histogram distributions and box-and-whisker plots of the gamma for the Taylor Creek sandstone/conglomerate and shale, and for the Jackass Mountain shale in the Honolulu Nazko A-4-L well.

The physical rock properties are summarized in Table 3.

Table 3: Statistical summary of the distribution of gamma ray activity, resistivity and velocity for the various lithology packages intersected in well A-4-L/93-B-11

Lithology		Gamma (API)		Resistivity (Ohm-m)		Velocity (km/s)	
		Mean	Median	Mean	Median	Mean	Median
Taylor Creek	Sandstone	2.70	2.69	349.73	285.94	4.89	4.95
	Shale	3.62	3.60	43.92	31.98	4.14	4.16
Jackass Mt		5.45	5.69	41.90	53.12	4.44	4.42

3.2.2.2 Bivariate Data Distributions

The cross-plots and 2D kernel density distributions of velocity-gamma and resistivity-gamma are presented in Figures 18 and 19, respectively. Here we look at the structure and relationships in the distributions of these data in the various rock units. The data in the scatter-plots are grouped into the units identified in Figure 14. There is no obvious relationship between velocity and gamma. However, in the kernel density distributions we see several clusters emerging that are related to lithology variations; clusters A and B belonging to the Taylor Creek sandstone and shale, respectively. There is a general decreasing trend in the velocity with increasing gamma ray activity in the Taylor Creek formations.

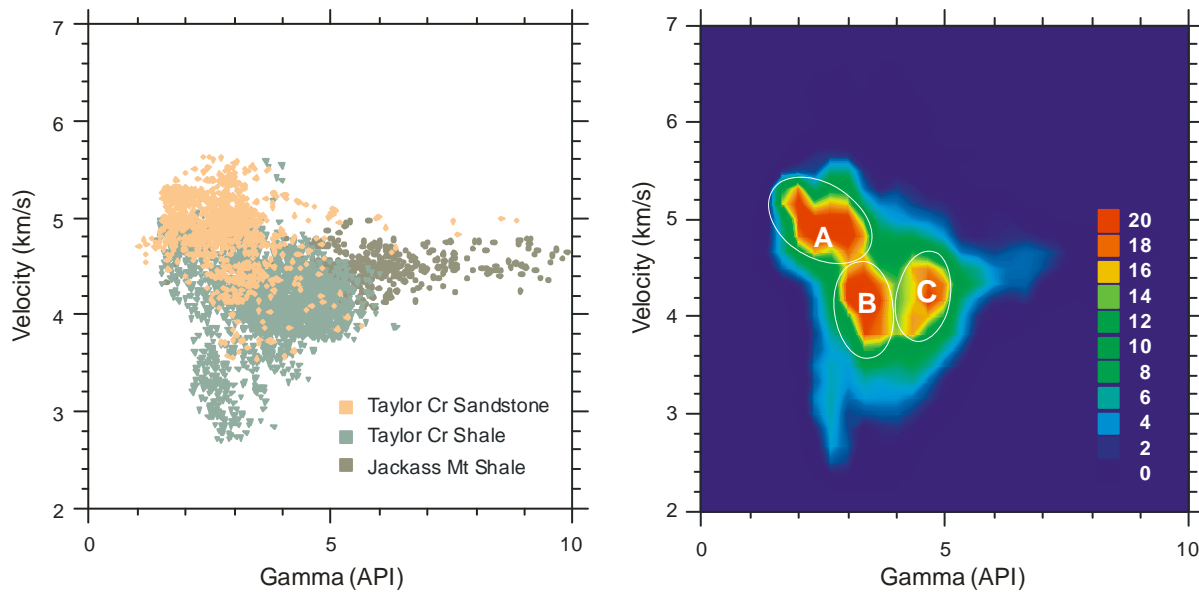


Figure 18. Velocity-gamma cross-plot and 2D kernel density distribution for data from A-4-L. Three clusters; A, B, and C are highlighted; A – Taylor Creek sandstone/ conglomerate; B- Taylor Creek shale; C – Jackass Mountain shale.

The resistivity-gamma cross-plot also does not reveal any relationship between these properties (Figure 20) and no significant clusters that can be related to shales or sandstone

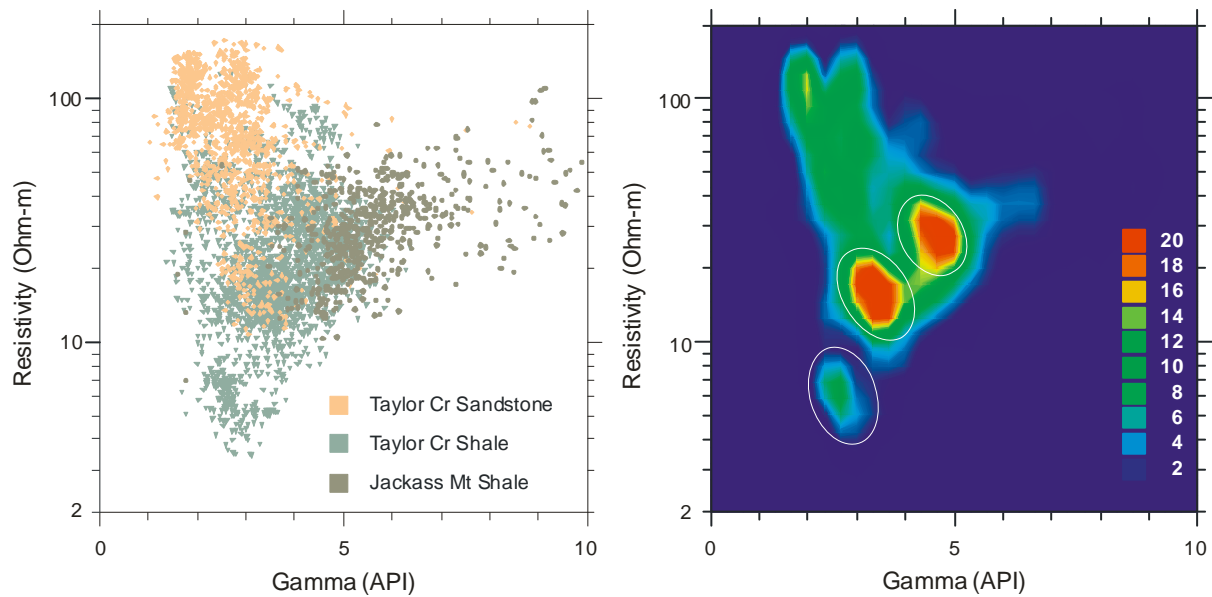


Figure 19. Cross-plot and 2D kernel density distribution of resistivity (logarithmic scale) versus gamma. Highlighted clusters show data concentrations.

3.2.3. Electrical and Acoustic Properties

In Figure 20 we have a cross-plot and kernel density distribution of resistivity versus velocity for dataset in well A-4-L. The lithology through which the well logs were acquired comprises sandstone and shales of the Taylor Creek and Jackass Mountain Formations. The correlation between resistivity and velocity is excellent. A log-linear regression of resistivity and velocity fits the dataset quite well but a better fit appears to a bit more complex curvilinear relationship.

$$\log_{10} (R) = -1.1432 + 0.5971 * V$$

$$\log_{10} (R) = -0.2548 + 0.3006 * V - 0.074 * V^2 + 0.0064 * V^3$$

Where R is the resistivity and V is the velocity.

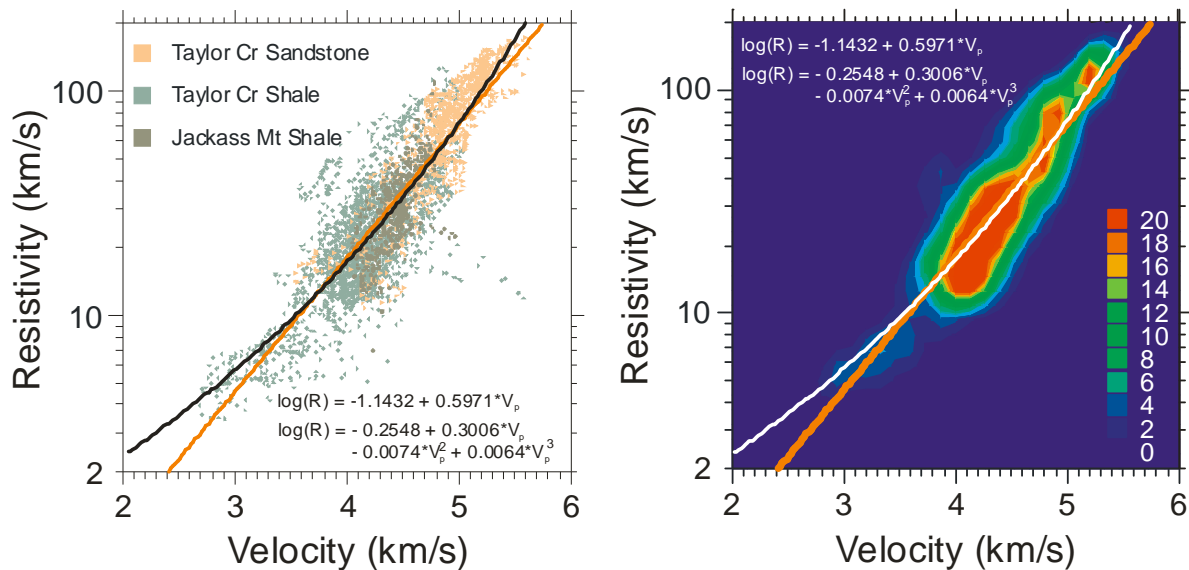


Figure 20. Resistivity-velocity cross-plot and 2D kernel density distribution for the Taylor Creek sandstone and shales and the jackass Mountain shale. A log-linear regression line (orange on both the cross-plot and kernel density distribution) and a more complex curvilinear relationship are presented on the figure.

3.3. Hudson's Bay Redstone C-75-A/93-B-4

3.3.1. Geophysical Characteristics of Lithology

Almost all the lithologies intersected in C-75-A are sedimentary rocks (Report on Hudson's Bay Redstone Well Report 630, 1960). The bottom of the well (1015 - 1300 m) is dominated by shale, siltstone and lesser sandstone. Two cherty sandstone sections are intersected from 1015 to 930 m and from 785 to 880 m. The upper part of the well (113 -630 m) comprises tuffaceous conglomeratic sandstone (Figure 21).

All the lithologies are clearly identified in the gamma ray, resistivity and velocity logs. The shales exhibit higher gamma activity, and lower resistivity and density whereas the sandstones and conglomerates exhibit relatively lower gamma activity and fairly high resistivities and velocities. The resistivity and velocity of the shales near the bottom of the well increase towards the bottom. This response may be due to decreasing porosity as recrystallized sandstone is prevalent in this section (Well report 630, 1960).

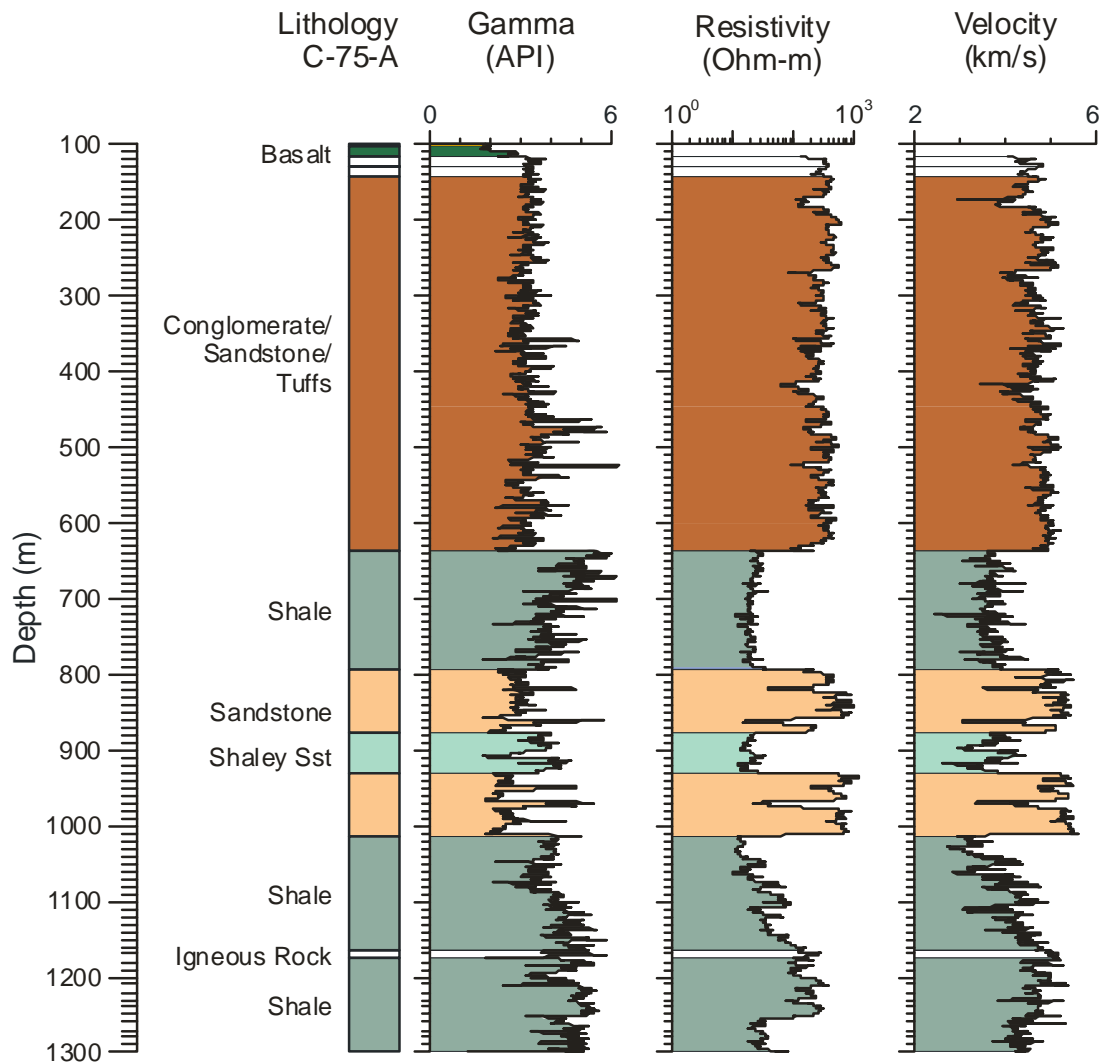
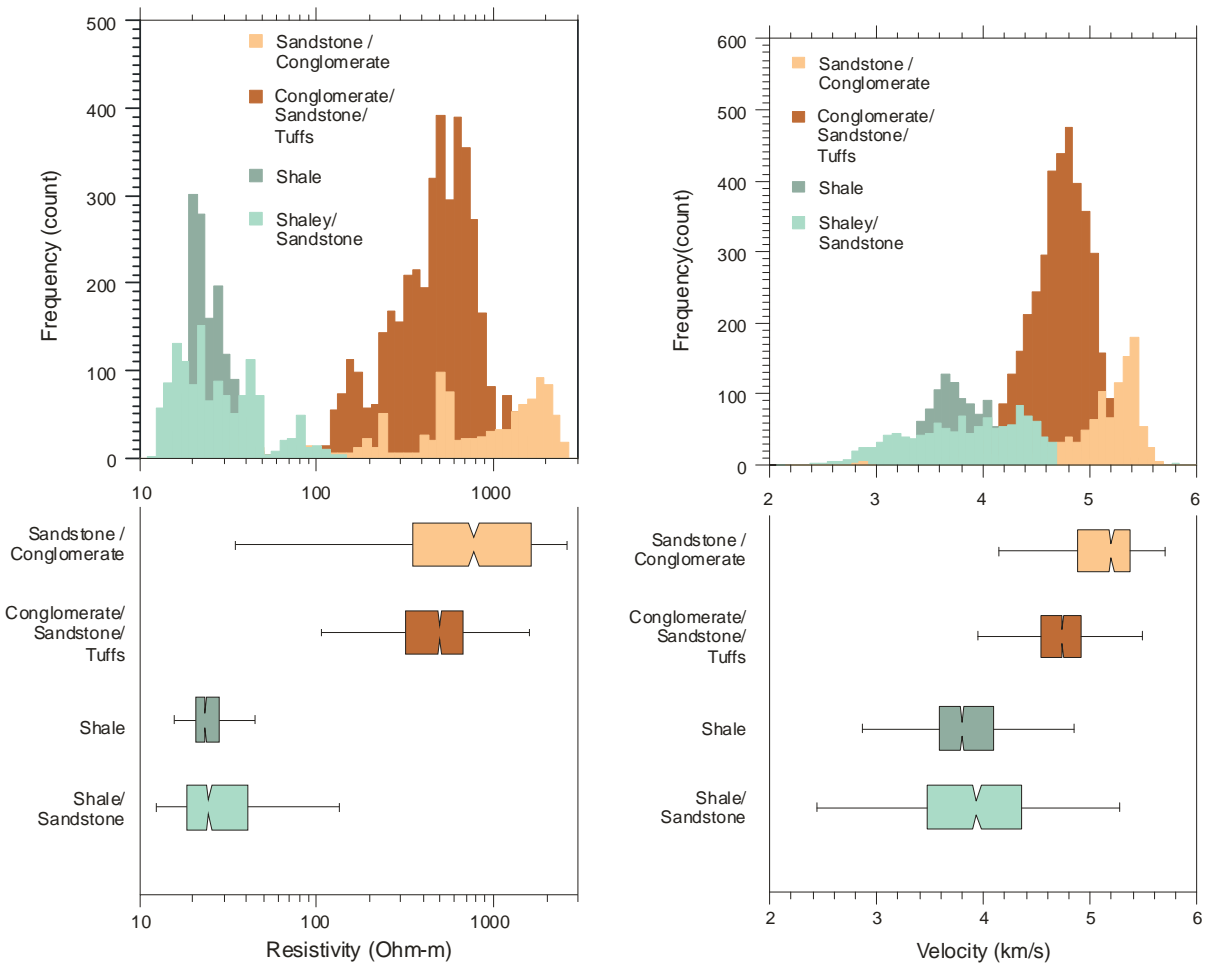


Figure 21. Gamma, resistivity and velocity logs acquired in the Hudson's Bay Redstone C-75-A well.

3.3.2. Physical Rock Property Distributions

3.3.2.1. Univariate Data Distributions

Histograms and box and whiskers plots showing distributions of resistivity and velocity in four lithology packages are presented in Figure 22. The resistivity data shows shales being distinctly different from the sandstone/conglomerates; the shales have resistivities around 20 ohm-m whereas the sandstone/conglomerates have resistivities greater than 400 ohm-m (Table 4). The velocity shows a similar distribution (Figure 22b), higher velocities being observed in the sandstone/conglomerates and lower velocities in the shales



Figures 22. Histogram distributions and box-and-whiskers plots of resistivity in logarithmic scale (a) and velocity (b) for sedimentary rocks in C-75-A/93-B-4.

Table 4: Statistical summary of the distribution of resistivity, velocity and gamma ray activity, for the shales and sandstone/conglomerates in well C-75-A/93-B-4

Lithology	Resistivity		Velocity		Gamma	
	Median	Mean	Median	Mean	Median	Mean
Conglomerate/ Sandstone/ Tuffs	293.784	296.389	4.776	4.756	10.699	10.680
sandstone conglomerate	474.096	477.379	5.184	5.017	10.274	10.432
Shale	21.979	24.365	3.806	3.850	11.753	11.720
Shale Sandstone	23.607	33.071	3.925	3.887	11.489	11.462

3.3.2.2. Bivariate Distributions

The resistivity-gamma and velocity-gamma cross-plots and 2D kernel density distributions are presented in Figures 23 and 24, respectively. The resistivity-gamma distribution appears to be an excellent discriminator of lithology (Figure 23). Two clusters are clearly identified in the kernel density distribution; cluster A comprising sandstone and conglomerates and cluster B comprising the shales. There is no obvious relationship between resistivity and gamma. Within the sandstones and conglomerates, there is a slight indication of decreasing resistivity with increase in gamma ray, probably due to increasing clay content.

The velocity-gamma field (Figure 24) does not characterise the shales and sandstones but there is a general trend of decreasing velocity with increasing gamma ray activity primarily due to increasing clay content.

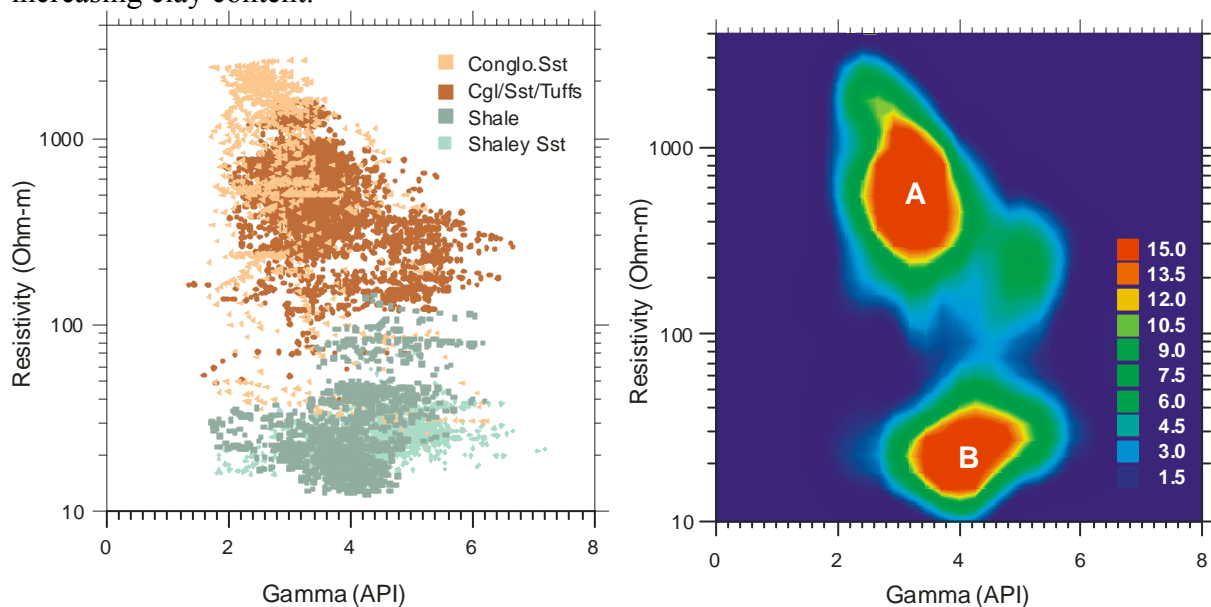


Figure 23. Resistivity-gamma cross-plot and 2D kernel density distribution for Hudson's Bay Redstone well C-75-A

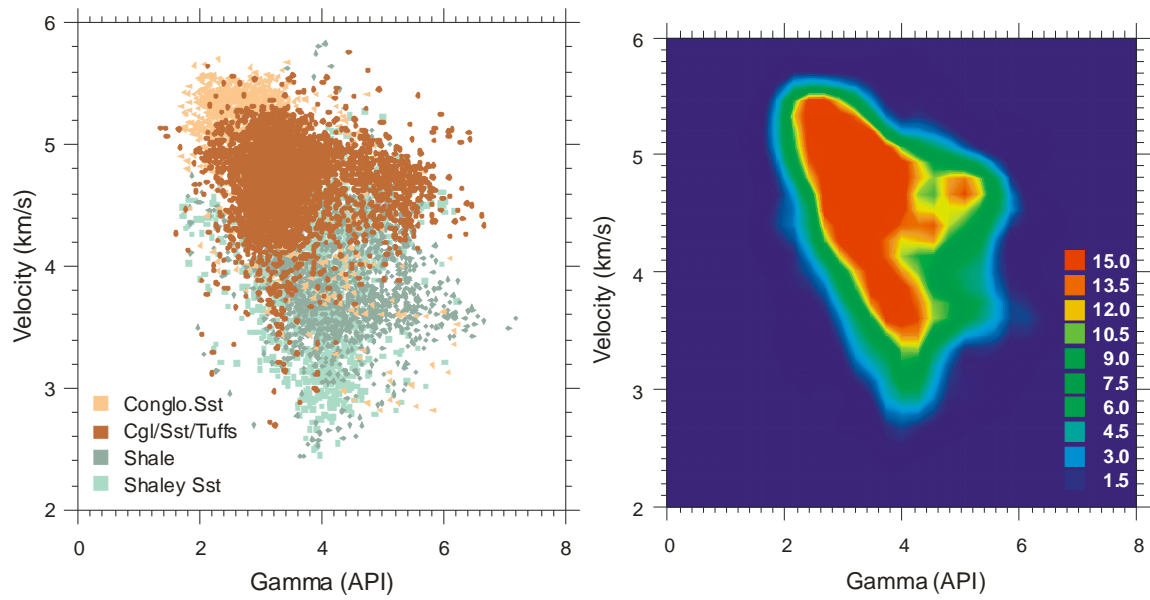


Figure 24. Velocity-gamma cross-plot and 2D kernel density distribution for Hudson's Bay Redstone well C-75-A.

3.3.3. Electrical and Acoustic Properties

Resistivity as a Function of Velocity

The resistivity-velocity relationship for the dataset in well C-75-A is shown in the cross-plot and 2D kernel density distribution (Figure 22). In general, resistivity increases as velocity increases, with a fairly good log-linear fit to the data. There are two distinct clusters in the dataset: one belonging to the shales (B) and one to the sandstone/conglomerates (A). A log-linear fit to the shale cluster gives the following relationship.

$$\log_{10} (R) = -0.754 + 0.168 * V_p$$

This relationship is quite different from that established in the shales of the Taylor Creek and Jackass Mountain Formation in well A-4-L. No explanation is currently available at the moment but it appears that there may be some mineralogical differences between the shales in these two wells.

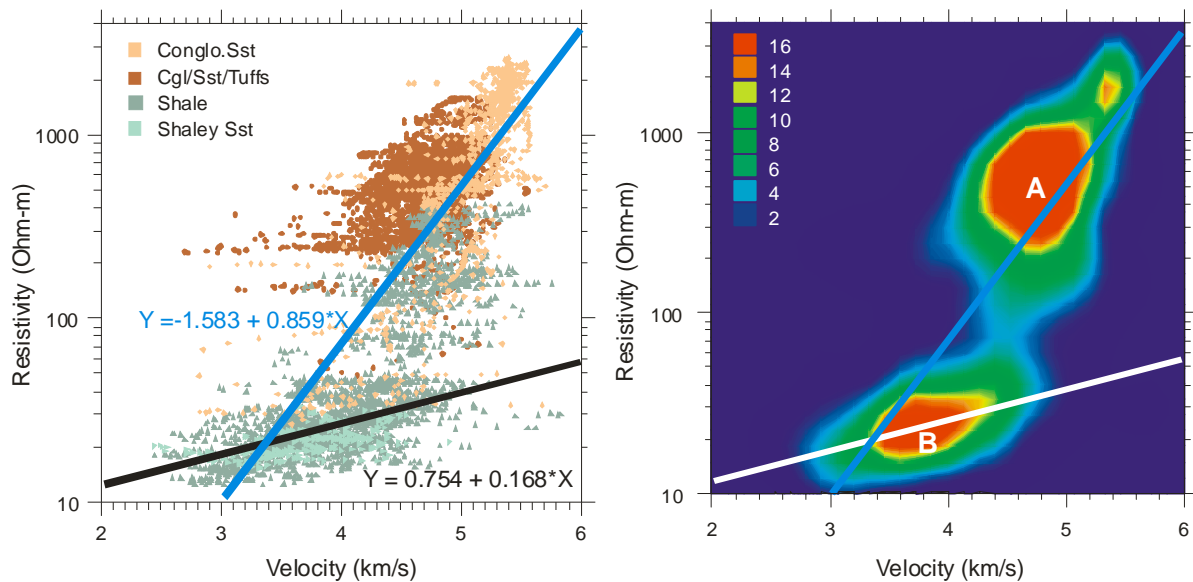


Figure 22. Resistivity-velocity cross-plot and 2D kernel density distribution for Hudson's Bay Redstone well C-75-A. Log-linear regression fit to the all the data (blue line) and log-linear fit to shales with resistivities <70 ohm-m (Black line – cross-plot, white line-kernel density plot)

4. Conclusions

The analysis of these well log data from the Nechako Basin indicates there are significant differences between the volcanics and sedimentary rocks in all the physical rock properties. These include gamma, porosity, resistivity, density, velocity and acoustic impedance. The reflection coefficients in both the resistivity and acoustic impedance are significant enough to allow fairly accurate imaging of the sedimentary rock sequences that are the potential hosts of oil and gas reserves.

Empirical relationships between velocity-density, resistivity-density, resistivity-velocity have been established. In situations where all the parameters are not available, it is now possible to derive the missing parameters from the relationships that have been established. These relationships indicate that geological models generated from seismic, electrical (e.g., MT) or gravity datasets would be comparable.

5. Acknowledgements

All well log data were acquired from Divestco through a subscription to their web based well log and production report delivery system – EnerGISite.com. Lithologies of the wells were acquired from the BC Ministry of Energy, Mines and Petroleum Resources, Oil and Gas division web site, <http://www.empr.gov.bc.ca/OG/oilandgas/petroleumgeology/WellReports/Pages/default.aspx>.

6. References

- Brocher, T.M. 2005. Empirical Relations between Elastic Wave speeds and Density in the Earth's Crust. *Bulletin of the Seismological Society of America*, Vol. 95, No. 6, pp. 2081–2092, December 2005, doi: 10.1785/0120050077.
- Divestco – EnerGISite.com, 2007. <http://www.energisite.com/> - a web based well log and production report delivery system from Divestco (<http://www.divestco.com> - 200, 1223 - 31st Ave NE, Calgary, Alberta, T2E 7W1).
- Eaton, D.W., Milkerit, B and Salisbury, M., 2003. Seismic methods for deep exploration: Mature technologies adapted to new targets. *The Leading Edge*, June 2003, pp. 580-585.
- Ferri, F. and Riddell, J. 2006. The Nechako basin project: new insights from the southern Nechako basin *in* British Columbia Ministry of Energy, Mines and Petroleum Resources, Summary of Activities 2006, pp. 89-124.
- Mwenifumbo, C.J. 1993. Kernel Density Estimation in the Analysis and presentation of Borehole Geophysical Data. *The Log Analyst*, Vol. 34, No. 5, pp.34-45
- Osadetz, K.G., Stasiuk, L.D., Evenchick, C.A., Ferri, F., Jiang, C., Thorsteinsson, E., and Wilson, N.S.F. 2006. Reservoirs, Petroleum Systems and Exploration in the Intermontane Basins of British Columbia. CSPG-CSEG-CWLS Joint Convention, Calgary, Alberta. Abstracts, pp.667-678, 2006. Available at <http://www.geoconvention.org/technical.asp> as of 6/12/2006
- Well History Report on Hudson's Bay Redstone C-75-A/93-B-4, Well Report 630. August 31, 1960
(<http://www.empr.gov.bc.ca/OG/oilandgas/petroleumgeology/WellReports/Pages/AMOCOREDSTONE.aspx>)
- Well History Report on Honolulu A-4-L/93-B-11. February 20, 1961
(<http://www.empr.gov.bc.ca/OG/oilandgas/petroleumgeology/WellReports/Pages/HONOLULUNAZKO.aspx>).
- Well History report on Canadian Hunter Nazko B-16-J/93-B11, British Columbia. Prepared for: Canadian Hunter Exploration, Ltd. By Donald T. Cosgrove, P. Geol., Consulting Geologist, June, 1981
(<http://www.empr.gov.bc.ca/OG/oilandgas/petroleumgeology/WellReports/Pages/CANHUNTERESSONAZKOB.aspx>).
- Well History report on Canadian Hunter Nazko D-96-E, British Columbia. Prepared for: Canadian Hunter Exploration, Ltd. By Donald T. Cosgrove, P. Geol., Consulting Geologist, March, 1981
(<http://www.empr.gov.bc.ca/OG/oilandgas/petroleumgeology/WellReports/Pages/CANHUNTERETALNAZKO.aspx>).